Clays and Clay Minerals, Vol. 37, No. 5, 439–445, 1989.

EFFECTS OF DRY GRINDING AND LEACHING ON THE CRYSTAL STRUCTURE OF CHRYSOTILE

HELÈNÉ SUQUET
Laboratoire de Réactivité de Surface et Structure, U.A. 1106 CNRS
Université Pierre et Marie Curie, 4 Place Jussieu
75252 Paris Cedex 05, France

Abstract—The structural damage produced by dry grinding and acid leaching of chrysotile was studied by transmission and scanning electron microscopy, infrared spectroscopy, X-ray powder diffraction, and thermogravimetric analysis. Severe dry grinding converted the chrysotile fibers into fragments having strong potential basic reaction sites. These sites were immediately neutralized by molecules present in the atmosphere (e.g., H_2O, CO_2). Acid leaching transformed the chrysotile fibers into very porous, non-crystalline silica, which was easily fractured into short fragments. The damage produced in the chrysotile structure by grinding or leaching was assessed by monitoring the intensity of various infrared absorption bands.

Key Words—Acid leaching, Asbestos, Chrysotile, Dry grinding, Infrared spectroscopy, Thermal gravimetric analysis, Transmission electron microscopy.

INTRODUCTION

Polycyclic aromatic hydrocarbons present in cigarette smoke are apparently adsorbed on asbestos fibers (chrysotile, crocidolite, etc.), and thereby strongly increase the risk of bronchopulmonary cancer for smokers exposed to asbestos (Selikoff *et al.*, 1968, 1980). Selikoff's findings have led several researchers to study the adsorption properties of various asbestos materials for such organic compounds (Harrington and Smith, 1964; Roe *et al.*, 1966; Fournier and Pézerat, 1982, 1986). Suquet (1989) recently described the importance of the surface state of chrysotile on the adsorption properties of this mineral. She noted that two samples of chrysotile from the same locality (Zimbabwe, formerly Rhodesia), both supplied by l'Union Internationale Contre le Cancer (UICC), exhibited quantitatively different adsorption properties, although they were highly similar in most chemical and structure properties. For example, one sample adsorbed 12 times less phenanthrene and 45% less CO_2 than the other.

Differential thermal analysis (DTA) showed that both samples dehydroxylated in two steps, but that the chrysotile sample having the weaker adsorption properties had a much larger low-temperature dehydroxylation peak than the other. Because grinding and/or acid leaching increased the size of this low-temperature dehydroxylation peak, she concluded that one of the samples had apparently been ground more and/or leached by the UICC during the defibrillation processes used to prepare these samples.

To assess the structural damage produced by grinding and acid leaching of chrysotile and to study the surface state of ground and leached products, several samples of chrysotile were dry-ground in an agate mortar or in a rotary ball mill or leached with oxalic or hydrochloric acid. The products were examined by means of X-ray powder diffraction (XRD), transmission (TEM) and scanning electron microscopy (SEM), infrared spectroscopy (IR), and thermal gravimetric analysis (TGA).

MATERIALS AND METHODS

Materials

A chrysotile sample from Eastern Transvaal (Republic of South Africa) was chosen as a reference material. It was cut into 2-cm long fibers with scissors, carefully defibrillated in water with a cutter-mixer for 4 min, and then freeze-dried. Inasmuch as the DTA curves of the original and the defibrillated materials were similar, crushing in water appeared to be a satisfactory means of defibrillating the sample without altering its surface properties. Several degraded chrysotile products were also examined, including:

1. Rhodesian chrysotile-2, supplied by UICC. This sample was shown by Suquet (1989) to give two dehydroxylation peaks, related to two types of OH surface groups, possibly caused by a UICC surface treatment.
2. Rhodesian chrysotile-2, intensely hand ground in an agate mortar (200 mg, 15 min). This sample was converted to a dark grey powder because of the homogeneous distribution of magnetite impurity during the grinding.
3. Eastern Transvaal chrysotile, dry ground in a rotary ball mill (1 g, 5 hr). This fibrous chrysotile was converted into a white powder.
4. Eastern Transvaal chrysotile, partially leached. This

Table 1. Chemical analyses (wt. %) of Transvaal chrysotile samples stored at 40% relative humidity.

	SiO_2	Al_2O_3	FeO	Fe_2O_3	CaO	MgO	Na_2O	K_2O	H_2O^1
Transvaal chrysotile	40.79	0.14	0.57	0.76	0.98	41.45	0.08	0.03	15.19
Rhodesian chrysotile	38.18	1.09	0.39	2.21	0.28	42.24	0.11	—	15.45
Theoretical $Mg_3Si_2O_5(OH)_4$	43.37					43.62			12.99

[1] Weight loss at 1030°C.

sample was prepared by treating it for 48 hr at room temperature with oxalic solution (0.05 mole/liter, unstirred) (Thomassin *et al.*, 1977).

5. Eastern Transvaal chrysotile, totally leached. This material was prepared by treating it for 2 hr at 90°C with 6 N HCl (1 mg, 300 ml).

The degree of leaching (i.e., the ratio of extracted Mg vs. initial Mg) was calculated to be about 20% for the partially leached sample and 100% for the totally leached sample. All samples were stored at 40% relatively humidity (RH).

A comparison of the chemical analyses of the samples (Table 1) indicates more Al-for-Si substitution in the Rhodesian chrysotile that in the Transvaal chrysotile; however, the Fe-for-Mg substitution is greater in the latter material. The charge deficit is balanced by the presence of other cations (see Suquet *et al.*, 1987). Weight-loss values at 1030°C in air indicate that the Rhodesian chrysotile adsorbs slightly more water than the Transvaal chrysotile.

Both samples contained impurities: about 2.5% calcite in the Transvaal sample and about 2–2.5% magnetite and 1% magnesite in the Rhodesian sample. No trace of brucite, common in many asbestos samples, was detected by XRD, TEM, or IR in either sample.

Methods

The XRD patterns were obtained with a Siemens D500 diffractometer using filtered CuKα radiation. Randomly oriented specimens were prepared by packing freeze-dried material into a depression on a plastic slide. IR spectra were recorded using a double-beam Perkin-Elmer Spectrometer 580B. KBr discs were prepared from a fine mixture of 150 mg KBr and 1 mg sample. TGA was carried out under a N_2 stream at a heating rate of 10°C/min, using 5 mg of sample and a Perkin-Elmer TGA 7 Analyzer. TEM and SEM and associated selected-area electron diffraction (SAD) and energy-dispersive X-ray (EDX) patterns were obtained using a JEM-100CX II instrument. The fibers were first opened by an ultrasonic treatment applied to a water suspension of the sample. A drop of suspension was dried on a carbon-coated Cu grid. Because prolonged exposure to the electron beam damaged the chrysotile structure, thereby weakening and broadening the diffraction spots and buckling the fiber edges, the SAD patterns were photographed as quickly as possible, followed immediately by an electron micrograph of the sample.

RESULTS

Electron microscopy

SEM and TEM examinations showed that the fibers of both chrysotile samples were flexible. The electron diffraction patterns closely resembled those reported by Zussman and Brindley (1957) for chrysotile-2M_{c1}. The two samples differed in the length of the fibers; in the Rhodesian sample, the fiber length was inhomogeneous and ranged from 0.1 to 4 μm, and short fibers were attached to large particles of magnetite (Figure 1). In the Transvaal sample, the fiber length ranged from 0.5 to 1 μm.

The SEM and TEM images of both dry-ground samples were similar and indicated that grinding destroyed their fibrous morphology (Figure 2). Some fibrils having a crystalline structure remained, but they were short and contained new points of fracture on their edges. They gave electron diffraction patterns corresponding to a disordered powder; the diffraction spots from the individual layers were distributed along the arcs of a circle. The fractures were perpendicular to the fiber axis (*a*). The short fibrils appeared to be cemented by shapeless, noncrystalline material. These same features were observed by Papirer and Roland (1981) for a Canadian chrysotile ground for 30 hr in toluene. These features explain the decrease in surface area and the

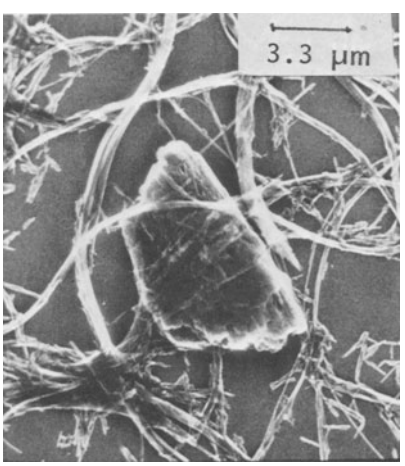

Figure 1. Scanning electron micrograph of Rhodesian chrysotile; short fibers are attached to a magnetite particle.

https://doi.org/10.1346/CCMN.1989.0370507 Published online by Cambridge University Press

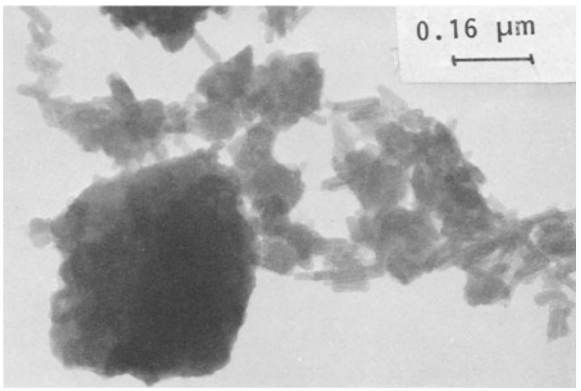

Figure 2. Transmission electron micrograph of dry-ground Transvaal chrysotile.

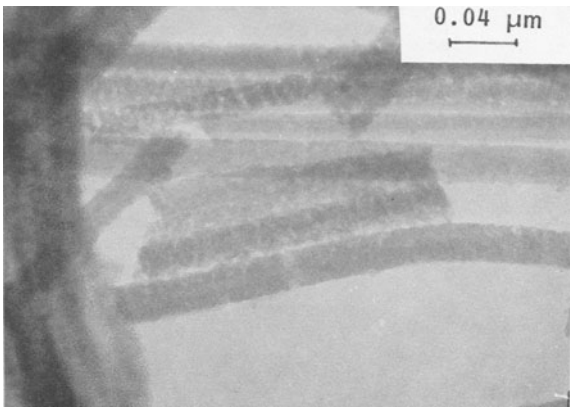

Figure 3. Transmission electron micrographs of 100% leached Transvaal chrysotile showing its porous morphology.

increase in the amount of Mg that was extracted from the chrysotile surface. The EDX spectrum of the ground Transvaal sample showed that the Mg:Si ratio (0.84) of the short fibrils was less than that of the original material (1.00). This ratio was slightly less (0.76) for the shapeless, noncrystalline material, suggesting a release of Mg from the severely distorted and strained structure.

SEM and TEM examinations of the totally leached Transvaal chrysotile showed that the fibrils were cracked and completely porous (Figure 3). No distinct SAD patterns could be obtained, indicating that the residue of the severe acid attack was noncrystalline. The EDX spectrum showed strong Si peaks, suggesting that this noncrystalline material is chiefly silica, thereby corroborating Fripiat and Mendelovici (1968) and Pacco *et al.* (1976). A small Mg peak was also observed, probably due to the presence of a few incompletely leached fibers. The Rhodesian chrysotile was more affected by the acid attack than the Transvaal chrysotile. In Figure 4, porous fibers, porous small fragments, and a shapeless material are all present. The coexistence of these three morphologically different materials is probably related to the inhomogeneous fiber lengths in the untreated sample.

X-ray powder diffraction patterns

XRD analysis indicated that the Transvaal sample was chiefly clinochrysotile (chrysotile-$2M_{cl}$) and that the Rhodesian sample was a mixture of clino- and orthochrysotile (chrysotile-Or_{cl}), the monoclinic form being the major component. The unit-cell parameters of the monoclinic form in both samples are:

	a (Å)	*b* (Å)	*c* (Å)	β (°)
Transvaal	5.27(1)	9.18(2)	14.59(3)	92.33(8)
Rhodesian	5.31(1)	9.22(2)	14.63(3)	92.79(8)

Wicks and O'Hanley (1988) pointed out that Al and Fe^{3+} usually substitute for Mg and Si, thereby relieving some of the misfit between the tetrahedral and octahedral sheets, even if Mg is replaced by Fe^{2+}. The chemical analyses in Table 1 suggest that the larger cell parameters (0.2 to 0.7%) of the Rhodesian chrysotile are mainly due to its Al content, which is eight times greater than that of the Transvaal chrysotile.

The XRD patterns in Figure 5 indicate that major structural changes took place on grinding and leaching. The basal spacings of the ground Transvaal chrysotile were less intense (particularly the 002 and 004 reflections) due to the fragmentation of the fibers, which took place essentially along the *c* axis. The 20*l* and 060 reflections were less affected because the crystal, in the *b* direction, retained a length of about 0.1 μm and consequently gave sharp Debye-Scherrer patterns. The broadening of the reflections and the appearance of a band at about 3.96 Å were apparently due to the noncrystalline material observed by TEM. The XRD pattern of the leached Transvaal sample showed only some of the principal chrysotile reflections, suggesting that

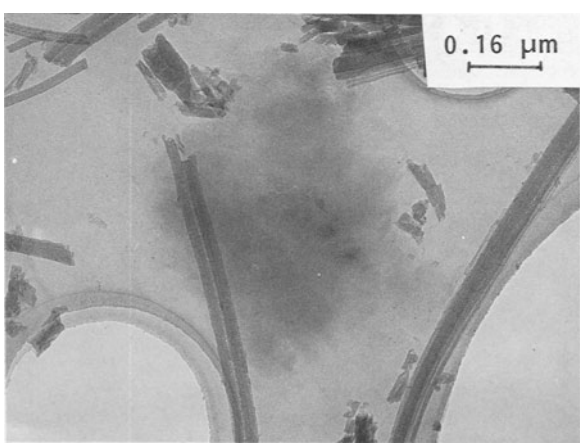

Figure 4. Transmission electron micrograph of 100% leached chrysotile showing three morphological features based on the primitive fiber length: porous fibers, porous short fragments, and a shapeless material.

https://doi.org/10.1346/CCMN.1989.0370507 Published online by Cambridge University Press

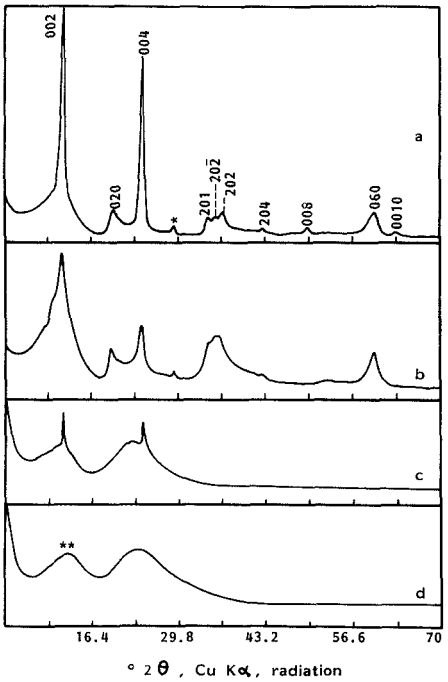

Figure 5. X-ray powder diffraction patterns of (a) Transvaal chrysotile (b) dry-ground Transvaal chrysotile (c) 100% leached Transvaal chrysotile (d) Aerosil 380. * = calcite; ** = plastic peak of sample holder.

the chrysotile structure persisted to some degree. These reflections do not correspond to any of the silica phases (Figure 5d).

Infrared absorption

The use of IR spectroscopy for the identification and structural studies of chrysotile is well known (see, e.g., Farmer, 1974; Yariv and Heller-Kallai, 1975; Jolicoeur and Duchesne, 1981; Luys *et al.*, 1982). The IR absorption spectrum of the carefully defiberized Transvaal chrysotile is illustrated in Figures 6a (OH-stretching region) and 7a (lattice-vibration region). In the lattice-vibration region more absorption bands are present than have been reported in the literature, probably because this sample was prepared without altering its surface. The absorption maxima of the Transvaal chrysotile are listed in Table 2; the assignments for the main peaks are consistent with those of Luys *et al.* (1982). The weak absorptions at 1430, 872, 711, and 325 cm^{-1} correspond to the calcite impurity.

A comparison of the IR curves of the two chrysotile samples (Figures 6a, 6b, 7a, and 7b) shows that the Si–O absorption bands of the Rhodesian chrysotile are broad, particularly the 1025-cm^{-1} vibration, and that the intensities of the cation-oxygen vibrations at 655, 552, 475, and 403 cm^{-1} are weaker and that at 417 cm^{-1} stronger than those of the Transvaal chrysotile. These results support the DTA data of Suquet (1989), which suggested damage to the crystalline structure of the Rhodesian chrysotile. They also indicate that IR absorption bands are highly sensitive to the effect of surface treatments.

The IR spectra of both dry-ground chrysotile samples show that the different comminution treatments (hand-grinding and ball-milling) strongly disrupted the structure (Figures 6c and 7c). In these spectra, the three components of the ν_3 mode of SiO_4 are coalesced, and two broad, diffuse bands are present at 1060 and 987 cm^{-1}. The weak absorption bands (655, 552, 475, and 403 cm^{-1}) in the Transvaal chrysotile spectrum cannot be distinguished, and the sharp bands at 605, 432, and 302 cm^{-1} are broad and their maxima are commonly shifted (615 and 442 cm^{-1}). Some new bands can be seen at 550, 458, and 380 cm^{-1}, suggesting the presence of a new phase in the sample. The absorption at 458 cm^{-1} indicates the presence of noncrystalline silica.

Table 2. Infrared absorption bands of Transvaal chrysotile.

	Vibrational frequency	Assignment
Hydroxyl group	3700 vs	External OH-stretching vibration
	3651 m	Internal OH-stretching vibration
	3450 br	Stretching vibration of physisorbed water
	1635 br	Bending vibration of physisorbed water
	1082 s	Out-of-plane Si–O stretching vibration
	1025 s	In-plane Si–O stretching vibration
	960 s	Asymmetric stretching vibration of Si–O
	655 w, sh	In-plane stretching mode of the Mg octahedra
	605 s, br	
	552 w	Out-of-plane bending mode of Si–O
	475 w, br	Out-of-plane bending mode of the Mg octahedra
	435 s	
Lattice vibrations	417 vw	
	403 m	Si–O and Mg–O bending modes
	385 i	
	302 m	Mg–O bending mode

w = weak; v = very; br = broad; sh = shoulder; i = inflection. The weak absorption bands at 1430, 872, 711, and 325 cm^{-1} correspond to calcite impurity.

https://doi.org/10.1346/CCMN.1989.0370507 Published online by Cambridge University Press

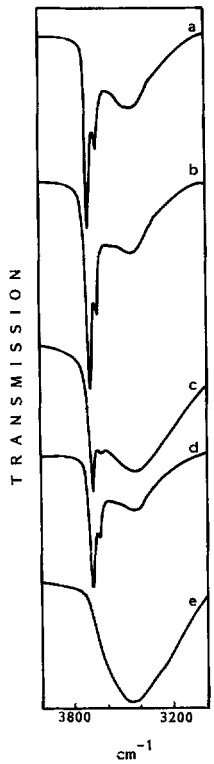

Figure 6. Infrared spectra of the OH-stretching region for chrysotile fibers stored at 40% relative humidity as a function of surface treatments: (a) Transvaal chrysotile (b) Rhodesian chrysotile (c) dry-ground Transvaal chrysotile (d) partially leached chrysotile (e) 100% leached chrysotile.

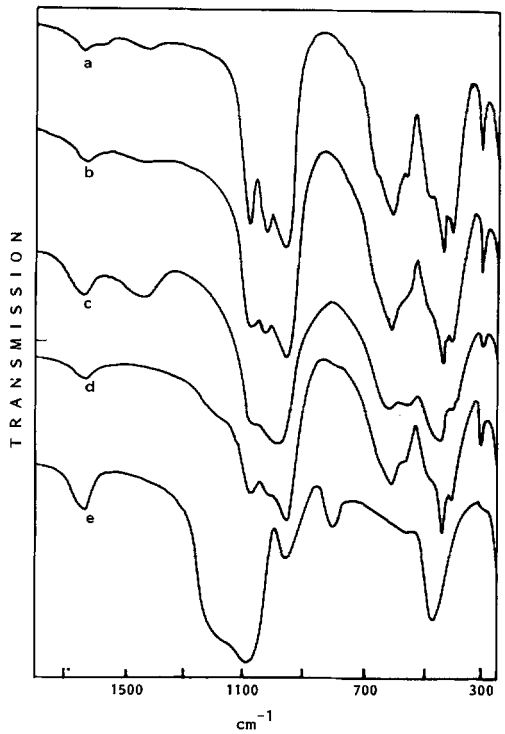

Figure 7. Infrared spectra of the lattice region for chrysotile fibers stored at 40% relative humidity as a function of surface treatments: (a) Transvaal chrysotile (b) Rhodesian chrysotile (c) dry-ground Transvaal chrysotile (d) partially leached chrysotile (e) 100% leached chrysotile.

The persistence of the absorption bands at 302, 400, and 442 cm^{-1} indicates, however, that the basic structure remained to some degree, inasmuch as these bands are not part of the IR spectrum of noncrystalline silica of magnesia.

Unlike the lattice vibrations, the OH-stretching vibrations were not greatly affected by the grinding treatment, inasmuch as short-range order was present. Moreover, the frequencies of the OH vibrations are characteristic of free OH groups, suggesting that adjacent hydroxyl groups were not coupled. The IR spectra of both dry-ground chrysotile samples show a broad diffuse band at about 1430 cm^{-1} and an increase in intensity of the 3440- and 1630-cm^{-1} absorption bands. Inasmuch as the 1430-cm^{-1} band is not present in the IR pattern of the unground Rhodesian sample and because the intensity of this band increased markedly after the grinding of the Transvaal sample (Figures 7a and 7c), this band is probably due to CO_2, which adsorbed on the surface of the chrysotile during the grinding. The increase in intensity of the 3440- and 1630-cm^{-1} absorption bands suggests an increase in the amount of physisorbed water. The comminution caused numerous dislocations perpendicular to the fibers, created highly reactive surface sites, and was able to fix molecules existing in the ambient atmosphere (e.g., CO_2 and H_2O). Suquet (1989) showed that CO_2 was sorbed on electron-donor sites derived from OH groups in low coordination at crystal edges and from external OH groups bearing a negative charge due to the presence of cationic substitution or vacancies.

The IR spectrum of the 20% leached chrysotile (Figures 6d and 7d) indicates the presence of some hydrated, noncrystalline silica in the sample because of (1) an increase of surface water (3440 and 1650 cm^{-1}); (2) a shoulder at 1200 cm^{-1} assigned to a free-silica stretching vibration; (3) a shoulder at about 800 cm^{-1} assigned to a Si–OH deformation band; (4) a decrease in intensity of the Mg–O vibrations at 655 and 475 cm^{-1}; and (5) a broadening of the Si–O vibrations at 1082, 1025, and 552 cm^{-1}. The mild acid attack partially solubilized the brucite sheet of the chrysotile and transformed the Si–O bands into Si–OH bands. The 100% leached chrysotile produced an IR spectrum that corroborates the breakdown of the structure and the transformation into hydrated silica (Figures 6e and 7e). OH-stretching vibrations are absent, and intense bands at 3440 and 1638 cm^{-1} indicate a large quantity of water physisorbed on Si–OH groups.

https://doi.org/10.1346/CCMN.1989.0370507 Published online by Cambridge University Press

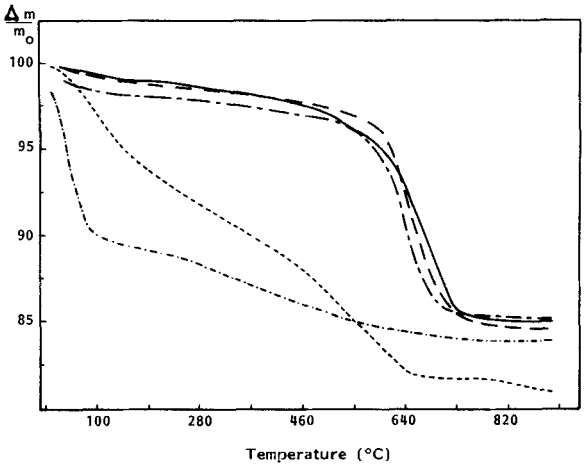

Figure 8. Weight loss of chrysotile fibers stored at 40% relative humidity as a function of temperature in N_2 heating 10°C/min): – – – = Transvaal chrysotile; —— = Rhodesian chrysotile; –·–·– = partially leached chrysotile, ----- = dry-ground Transvaal chrysotile; -·-·- = 100% leached chrysotile.

Thermogravimetric analyses

The fractional weight losses observed on heating in a N_2 stream chrysotile samples stored at 40% RH are shown in Figure 8 as a function of temperature. The Transvaal sample lost 0.5% weight on heating to 100°C, due to the evolution of physisorbed water from the surface and an additional 2% weight on heating to 470°C. This second loss was probably due to the removal of water either trapped in pores, as was suggested by Young and Healey (1954), or from the most loosely held OH groups (linked to Fe^{2+}). An additional 12.3% weight was lost on heating the sample from 590° to 910°C and can be attributed to dehydroxylation of the chrysotile to forsterite and noncrystalline silcia (Ball and Taylor, 1963; Brindley and Hayami, 1965; Hodgson, 1979). Calcite decomposed at >900°C (Mackenzie, 1957).

At 470°C the two chrysotile samples showed similar weight losses. Because the Rhodesian chrysotile contained some damaged fibers but not calcite (Suquet, 1989), this result suggests that presence of more sorbed water on this sample and indicates that part of this water was strongly held at surface sites. The TGA curve of the intensely ground chrysotile shows several inflections, suggesting successive dehydrations and the removal of CO_2. The noncrystalline, completely dehydroxylated product was formed at 650°C, whereas the same reaction occurred at 735°C for the untreated chrysotile. The TGA curve of the totally leached chrysotile showed about 10% weight loss <100°C, due to the expulsion of hygroscopic moisture, and an additional 6% weight loss on heating the material to 910°C. This second loss may have been due to the removal of water directly fixed on silanol groups.

SUMMARY AND CONCLUSIONS

Severe dry grinding converted chrysotile fibers into fragments cemented by a shapeless, noncrystalline material. This comminution treatment apparently broke atomic bonds and produced strong potential reaction sites, which were able to adsorb CO_2 and H_2O molecules from the atmosphere. Acid leaching transformed chrysotile into porous, noncrystalline hydrated silica, which easily fractured into short fragments. If the acid attack was too severe, these fragments converted into shapeless material.

This study has shown that: (1) The damage produced in the chrysotile structure by dry grinding or acid leaching may be assessed by monitoring the intensity of various IR absorption bands; some cation-oxygen vibrations (e.g., at 665, 552, 475, 403, and 302 cm^{-1}) appear to be highly sensitive to such treatments. (2) Pretreatment (defibrillation and/or leaching) may destroy or poison electron-donor surface sites of chrysotile and therefore affect the properties that involve surface phenomena (e.g., adsorption, dissolution, biologic reactivity). These results support those of Gronow (1987), who showed that a grinding and/or leaching pretreatment of chrysotile critically affects its dissolution in water.

ACKNOWLEDGMENTS

We thank M. Lavevrgne and P. Beaumier for performing the electron microscopic analyses and B. Imelik for his helpful comments.

REFERENCES

Ball, M. C. and Taylor, H. F. W. (1963) The dehydration of chrysotile in air and under hydrothermal conditions: *Miner. Mag.* **33,** 467–482.

Brindley, G. W. and Hayami, R. (1964) Kinetics and mechanisms of dehydration and recrystallization of serpentine: *Clays & Clay Minerals* **34,** 35–47.

Farmer, V. C. (1974) *The Infrared Spectra of Minerals:* Mineralogical Society, London, 342–348.

Fripiat, J. J. and Mendelovici, E. (1968) Dérivés des silicates. I—Le dérivé méthylé du chrysotile: *Bull. Soc. Chim. France* **2,** 483–492.

Fournier, J. and Pézerat, H. (1982) Mode d'adsorption des hydrocarbures polycycliques aromatiques sur les amiantes. Cas du phénanthrène: *J. Chim. Phys.* **79,** 589–596.

Fournier, J. and Pézerat, H. (1986) Studies on surface properties of asbestos. III—Interactions between asbestos and polynuclear aromatic hydrocarbons: *Environ. Res.* **41,** 276–295.

Gronow, J. R. (1987) The dissolution of asbestos fibers in water: *Clay Miner.* **22,** 21–35.

Harrington, J. S. and Smith, M. (1964) Studies of hydrocarbons on mineral dusts, the evolution of 3-4 benzopyrene and oils from asbestos and coal dusts by serum: *Arch. Environ. Health* **8,** 453–458.

Hodgson, A. A. (1979) *Chemistry and Physics of Asbestos:* in *Asbestos, Vol. 1,* L. Michaels and S. S. Chissick, eds., Wiley, New York, 83–110.

Jolicoeur, C. and Duchesne, D. (1981) Infrared and thermogravimetric studies of the thermal degradation of chrys-

otile asbestos fibers: Evidence for matrix effects: *Can. J. Chem.* **59,** 1521–1526.

Luys, M. J., Deroy, G., Vansant, E. F., and Adams, F. (1982) Characteristics of asbestos minerals: *J. Chem. Soc. Faraday Trans. 1,* **78,** 3561–3571.

Mackenzie R. C. (1957) *The Differential Thermal Investigation of Clays:* Mineralogical Society, London, 331–333.

Pacco, F., Van Gangh, L., and Fripiat, J. J. (1976) Etude par spectroscopie infrarouge et résonance magnétique nucléaire de la distribution homogène des groupes silanols d'un gel de silice fibreux: *Bull. Soc. Chim. France* **5,** 1021–1026.

Papirer, E. and Roland, P. (1981) Grinding of chrysotile in hydrocarbons, alcohol, and water: *Clays & Clay Minerals* **29,** 161–170.

Roe, F. J. C., Walters, M. A., and Harrington, J. S. (1966) Tumours initiation by natural and contaminating asbestos: *Int. J. Cancer* **1,** 491–495.

Selikoff, I. J., Hammond, E. C., and Churg, J. (1968) Asbestos exposure, smoking and neoplasma: *J. Amer. Med. Assoc.* **204,** 106–112.

Selikoff, I. J., Seidman, H., and Hammond, E. C. (1980) Mortality effects of cigarette smoking among amosite asbestos factory workers. *J. Natl. Cancer Inst.* **65,** 507–513.

Suquet, H. (1989) The differences between adsorption properties of two Rhodesian chrysotile samples. Relation between the DTA features introduced by leaching and grinding: *Can. J. Chem.* **67,** (in press).

Suquet, H., Malard, C., Fournier, J., and Pézerat, H. (1987) Capacité d'échange cationique et charge de surface du chrysotile: *Bull. Miner.* **110,** 711–715.

Thomassin, N., Goni, J. H., Touray, J. C., and Jaurand, M. C. (1977) An XPS study of the dissolution kinetics of chrysotile in 0.1 N oxalic acid at different temperatures. *Phys. Chem. Miner.* **1,** 385–398.

Wicks, F. F. and O'Hanley, D. S. (1988) Serpentine minerals: Structures and properties: in *Hydrous Phyllosilicates,* Reviews in Mineralogy, S. W. Bailey, ed., Miner. Soc. America, Washington, D.C., 113–114.

Yariv, S. and Heller-Kallai, L. (1975) The relationship between the IR spectra of serpentines and their structures: *Clays & Clay Minerals* **23,** 145–152.

Young, G. J. and Healey, F. H. (1954) The physical structure of asbestos: *J. Phys. Chem.* **58,** 881–884.

Zussman, J. and Brindley, G. W. (1957) Electron diffraction studies of serpentine minerals: *Amer. Mineral.* **42,** 133–153.

(Received 13 September 1988; accepted 1 January 1989; Ms. 1827)